Design Optimization of Feedforward Equalization for Mobile Fronthaul Based on Delta-Sigma Modulation With High-Order QAM Signals

Jianghao Li, Yangsheng Yuan, and Yangjian Cai

***Abstract*—Delta-sigma modulation can be used as a high spectral efficiency interface in place of conventional common public radio interface (CPRI) in mobile fronthaul (MFH) networks. However, inter-symbol interference (ISI) becomes more difficult to be mitigated in the networks due to bit quantization in delta-sigma modulation. In this paper, we propose a novel feedforward equalization (FFE) scheme based on the least mean square (LMS) algorithm for MFH networks employing 4th-order delta-sigma modulation technology with 1 and 2 bit quantization to alleviate the performance degradation caused by ISI. The performance of both 1-bit and 2-bit quantization systems employing the proposed FFE scheme with different tap lengths and step sizes has been systematically investigated. Our results show that, under the minimum computational complexity, the maximum transmission capacity can reach 8.98 Gbps when using the FFE scheme with 11 taps and step size of 3×10^{-5} or 3.5×10^{-5} and the average error vector magnitude (EVM) can be minimized to a level less than 0.032 with 19 taps and step size of 4×10^{-5} or 4.5×10^{-5} for 1-bit quantization system while for 2-bit quantization system, the maximum transmission capacity of 11.4 Gbps can be obtained when employing the FFE scheme with 19 taps and step size of 3.5×10^{-5} and the minimal average EVM less than 0.01 can be achieved with 19 taps and step size of 4×10^{-5}. More hopefully, this work provides guidelines for optimizing the equalization scheme based on the requirements of EVMs, capacity, and computational complexity.**

***Index Terms*—Radio-over-fiber, common public radio interface, mobile fronthaul, delta-sigma modulation, inter-symbol interference, feedforward equalization.**

I. Introduction

With the rapid rise of intelligent and ultra-wideband terminals and applications such as remote surgery, 4 K/8 K high-definition videos and virtual/augmented reality (VR/AR) in 5G and beyond, exponential growth of demands for data traffic are posing a great challenge with more strict requirements of higher capacity, lower latency, complexity and cost in mobile fronthaul (MFH) networks [1], [2]. Radio-over-fiber (RoF) technique is widely considered as a promising solution to the challenge where the radio signals transmitted from the centralized baseband unit (BBU) to the cell-site remote radio heads (RRHs) are achieved via optical fronthaul transmission links [3], [4]. Currently, RoF technique is mainly implemented in two major forms: analog radio-over-fiber (A-RoF) and digital radio-over-fiber (D-RoF). Compared to D-RoF, A-RoF has attracted more research attention in recent decade due to its inherent advantages of high spectral efficiency, high flexibility and low-complexity/cost implementation [5]. However, a nonnegligible shortcoming of A-RoF is the vulnerability to the noise and the signal impairments and distortion caused by fiber nonlinearity [6]. Despite D-RoF technique employing Common Public Radio Interface (CPRI) [7], [8], [9] is commonly considered as low bandwidth efficiency, which leads to the bottleneck of digital MFH to support massive mobile data transmission [10], theoretically it can achieve similar bandwidth efficiency as A-RoF under similar channel conditions, signal-to-noise ratios (SNRs) or error vector magnitudes (EVMs).

To realize bandwidth efficiency improvement for D-RoF and further increase the capacity of MFH networks, delta-sigma modulation technique was proposed for MFH networks [11], [12] where an analog-to-digital converter (ADC) with sampling rate much higher than conventional Nyquist ADC is applied to quantify the analog signals into digital ones, which enables the delivery of analog signals through digital ports and the data recovery of the received signals at RRHs using only a filters without expensive and high-linearity digital-to-signal converters (DACs) [13], [14]. Moreover, a unique advantage of the delta-sigma modulator is the functionalization of noise shaping which pushes the quantization noise out of the signal band [15]. Due to the aforementioned advantages, delta-sigma modulation technique has attracted extensive research interest and various study has been carried out such as the combination of hierarchical and delta-sigma modulations [16], ultra-high-order delta-sigma modulator [17] and novel feedback structures [18] to further improve the system performance and increase the transmission capacity in recent years.

Manuscript received 20 December 2023; accepted 26 December 2023. Date of publication 8 January 2024; date of current version 24 January 2024. This work was supported in part by the National Natural Science Foundation of China under Grants 12304325, 11974218, 11974219, 12174227, 12192254, and 92250304, and in part by the National Key Research and Development Program of China under Grants 2019YFA0705000 and 2022YFA1404800. *(Corresponding author: Jianghao Li.)*

The authors are with the Shandong Provincial Engineering and Technical Center for Light Manipulation and Shandong Provincial Key Laboratory of Optics and Photonic Devices, School of Physics and Electronics, Shandong Normal University, Jinan 250014, China, also with the Joint Research Center of Light Manipulation Science and Photonic Integrated Chip, East China Normal University, Shanghai 200241, China, also with the Shandong Normal University, Jinan 250014, China, and also with the East China Normal University, Shanghai 200241, China (e-mail: sdnuljhao@sdnu.edu.cn; yysheng@sdnu.edu.cn; yangjiancai@sdnu.edu.cn).

Digital Object Identifier 10.1109/JPHOT.2023.3348532

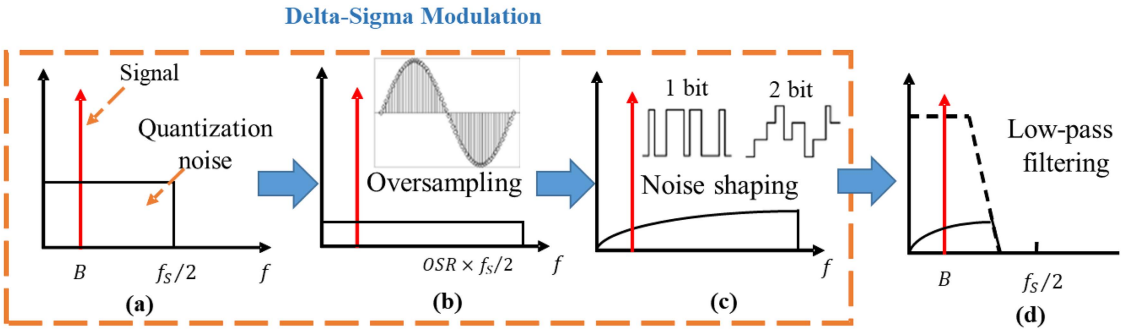

Fig. 1. Operation principle of (a) CPRI; (b)–(d) delta-sigma modulation scheme.

Nevertheless, to explore the benefits enabled by delta-sigma modulation, inter-symbol interference (ISI) needs to be eliminated via digital signal processing (DSP) since it's recognized as the main challenge to high-speed transmission systems. Otherwise, strong ISI can lead to performance degradation, wrong data recovery and even link outage. To solve the issue, equalizers based on feedforward or decision feedback architectures for delta-sigma in digital domain have been proposed and demonstrated [19], [20]. Despite, the proposed feedforward equalizers (FFEs) possess the advantage of low computational complexity, they fail to compensate the signal impairments caused by chromatic dispersion (CD) [21] via field information, which is attributed to the multipath effect when lightwave propagates along the fiber, since the original analog signals are usually quantified into intensity modulated (OOK or PAM-4) signals. To alleviate system performance degradation caused by ISI, a variety of equalization approaches such as constant modulus algorithm (CMA) [22], modified cascade multiple modulus algorithm (M-CMMA) [23], least mean square (LMS) [24], [25] and recursive least-square (RLS) [26], [27] equalization have been proposed for original high-order complex-valued signals and investigated extensively in recent decades. However, additional carrier phase estimation (CPE) employing the fourth power algorithm [28] within each equalization iteration is indispensable to recover the phase information of the received signals, which increases the computational complexity and the cost of training sequence significantly.

To further reduce the computational complexity of the FFE scheme for MFH networks employing delta-sigma modulation while preserving the capability of compensating CD-induced signal impairments, in this paper, we propose a novel FFE scheme based on LMS algorithm without CPE for improving the performance of MFH networks employing a 4th-order delta-sigma modulator with both 1-bit and 2-bit quantization. We systematically investigate the system performance using the proposed FFE scheme with different tap lengths and step sizes. The simulation results show that, for the lowest computational complexity, the maximum transmission capacity of 8.98 Gbps can be obtained for 1-bit quantization system when employing the FFE scheme with 11 taps and step size of 3×10^{-5} and 3.5×10^{-5} and the minimum average EVM less than 0.032 can be achieved with 19 taps and step size of 4×10^{-5} or 4.5×10^{-5}. Meanwhile, for 2-bit quantization system, the maximum transmission capacity can reach 11.4 Gbps with the proposed FFE scheme of 19 taps and step size of 3.5×10^{-5} and the minimal average EVM reaches below 0.01 when employing the proposed FFE scheme with lap length of 19 and step size of 4×10^{-5}.The study indicates the system performance can be improved significantly by employing FFE.

The rest of this paper is organized as follows: Section II presents the principles of delta-sigma modulation and our proposed feedforward equalization scheme. Section III illustrates the simulation setup and results. Section IV concludes the paper.

II. Principles of Delta-Sigma Modulation and Feedforward Equalization

A. Principle of Delta-Sigma Modulation

The operation principle of conventional CPRI is shown in Fig. 1(a), where Nyquist sampling scheme is employed. By contrast, in delta-sigma modulation scheme, the input analog signals are sampled with oversampling rate of

$$OSR = \frac{f_s}{2B} \tag{1}$$

where f_s is the sampling rate and B is the signal bandwidth. Consequently, the quantization noise is extended over a wide frequency area, which is shown in Fig. 1(b). After 1-or-2-bit quantization, the sampled signals are converted into on-off keying (OOK) or 4-level pulse amplitude modulation (PAM-4) signals. Meanwhile, noise shaping is performed to push the quantization noise out of the signal bandwidth. As shown in Fig. 1(c), the noise is mainly concentrated at the high-frequency domain while the signal is located at low-frequency domain. At the receiver, the original data stream can be retrieved from the quantified OOK or PAM-4 signals by filtering the quantization noise out of the signal bandwidth using a low-pass filter without digital-to-analog convertors (DACs) as shown Fig. 1(d).

The designed 4th-order delta-sigma modulator based on cascade-of-resonators feedforward (CRFF) structure is shown in Fig. 2(a), in which the reciprocal of the noise transfer function (NTF) can be expressed as

$$\frac{1}{NTF} = 1 + \frac{[(a+c)\,z - a]\left[z^2 - (2+e)z + 1\right] dz^2 - dz + fz^2}{(z^2 - 2z - bz + 1)\,(z^2 - 2z - ez + 1)} \tag{2}$$

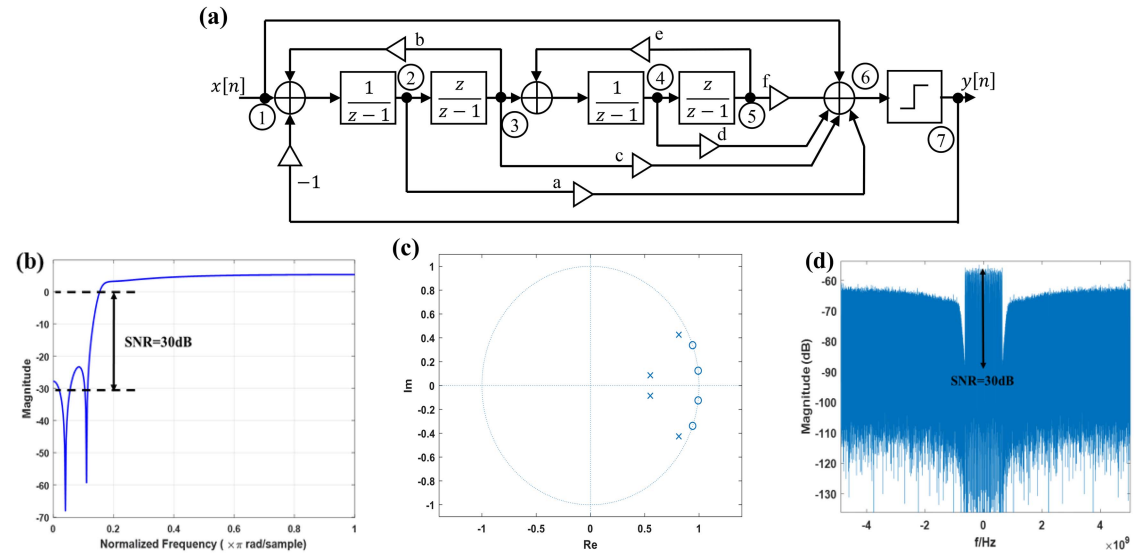

Fig. 2. (a) Z-domain block diagram; (b) NTF curve; (c) pole-zero diagram of 4th-order delta-sigma modulator; and (d) spectrum of the output of the delta-sigma modulator.

where $z = e^{2\pi f/f_s}$. *a-f* represent the feedback coefficients of the delta-sigma modulator, which can be obtained using R. Schreier's toolbox [29] or genetic algorithm [30], [31]. Based on the aforementioned principles, we obtain the NTF curve and the pole-zero diagram of the delta-sigma modulator which is illustrated in Fig. 2(b) and (c) respectively. Fig. 2(d) shows the spectrum of the output of the delta-sigma modulator. It can be observed from both NTF curve and the output spectrum that more than 30 dB SNR gain can be obtained by using the delta-sigma modulator, which enables the recovery of the received signals at low received optical power after filtering the quantization noise.

B. Principle of Feedforward Equalization

The quantized signal *R*(*t*) is firstly split into In-phase (I) and Quadrature (Q) sequences by a pair of orthogonal matched filters m_{I}(t) and m_{Q}(t), which can be written as

$$s_I(t) = R(t) \times m_I(t) = R(t)\cos(2\pi f_c t) \tag{3}$$

$$s_Q(t) = R(t) \times m_Q(t) = R(t)\sin(2\pi f_c t) \tag{4}$$

where f_c is the central frequency of the received signal spectrum. After band-pass filtering, the obtained data sequences are combined to recover the original high-order complex-valued signals, which can be expressed as

$$s(t) = H_{BPF}(t)R(t)\cos(2\pi f_c t) + jH_{BPF}(t)R(t)\sin(2\pi f_c t) \tag{5}$$

where $H_{BPF}(t)$ represents the responsitivity of the band-pass filter. Therefore, the recovered complex-valued signal in frequency domain is illustrated as

$$s(\omega) = 2\pi R(\omega)\left[H_{BPF}(\omega-\omega_c) + H_{BPF}(\omega+\omega_c)\right] \tag{6}$$

where $\omega_c = 2\pi\omega_c$.

Assume the pulse shape of the transmitted OOK or PAM-4 symbols can be defined as *g*(*t*) with amplitude of a_n and the symbol interval is T_s, then the transmitted symbols can be written as [32]

$$\begin{aligned} E(t) &= Ee^{-j\omega_0 t}V_c\cos(\omega_c t)\sum_{-\infty}^{\infty} a_n g\left(t-nT_s\right) \\ &= \frac{1}{2}EV_c\sum_{-\infty}^{\infty} a_n g\left(t-nT_s\right)\cdot\left[e^{j(\omega_c-\omega_0)t} + e^{-j(\omega_c+\omega_0)t}\right] \end{aligned} \tag{7}$$

where E and ω_0 represents the amplitude and the angular frequency of the electrical field of the lightwave, respectively. V_c and ω_c is the amplitude and the angular frequency of the RF clock. Assume only one symbol interval is considered for ease of calculation and analysis, then the transmitted signals in frequency domain can be expressed as

$$\begin{aligned} E(\omega) = \frac{1}{2}EV_c a_n \tau e^{-jn\omega T_s} &\cdot\left\{Sa\left[(\omega-\omega_f)\tau/2\right]e^{jn\omega_f T_s}\right. \\ &\left. + Sa\left[(\omega+\omega_p)\tau/2\right]e^{-jn\omega_p T_s}\right\} \end{aligned} \tag{8}$$

where $Sa(x) = \sin(x)/x$, $\omega_f = \omega_c$-ω_0 and $\omega_p = \omega_c$+ω_0. τ is the pulse width. After propagation in the fiber, the received signals can be expressed as

$$\begin{aligned} E_r(\omega) = \frac{1}{2}\mu EV_c a_n \tau e^{-j(n\omega T_s - \beta\omega_0 z_t)} &\cdot\left\{Sa\left[(\omega-\omega_f)\tau/2\right]e^{jn\omega_f T_s}\right. \\ &\left. + Sa\left[(\omega+\omega_p)\tau/2\right]e^{-jn\omega_p T_s}\right\} \end{aligned} \tag{9}$$

where μ is the amplitude attenuation coefficient. β and z_t represents the propagation constant and the transmission length in the

fiber. Then the received signals are detected by the photodetector (PD) with square-law detection, which can be expressed as

$$R(\omega) = \alpha |E_r(\omega)|^2 = \frac{1}{4}\alpha\mu^2 E^2 V_c^2 a_n^2 \tau^2 e^{-2j(n\omega T_s - \beta\omega_0 z_t)} \cdot \left\{ Sa\left[(\omega-\omega_f)\tau/2\right] e^{jn\omega_f T_s} + Sa\left[(\omega+\omega_p)\tau/2\right] e^{-jn\omega_p T_s} \right\}^2 \quad (10)$$

where α is the responsitivity of the PD. Substitute (10) into (6), the final expression of the recovered signal in frequency domain can be written as

$$s(\omega) = \frac{\pi}{2} H_{BPF}(\omega)\alpha\mu^2 E^2 V_c^2 a_n^2 \tau^2 \left[H_{BPF}(\omega-\omega_c) + H_{BPF}(\omega+\omega_c)\right] \cdot \left\{ Sa\left[(\omega-\omega_f)\tau/2\right] e^{jn\omega_f T_s} + Sa\left[(\omega+\omega_p)\tau/2\right] \times e^{-jn\omega_p T_s} \right\} e^{-j(n\omega T_s - \beta\omega_0 z_t)} \quad (11)$$

We can further write (10) as

$$s(\omega) = \tau S_a(\omega\tau/2) \cdot H(\omega) \quad (12)$$

where $H(\omega)$ is the transfer function that results in ISI in the system because of CD. To eliminate ISI caused by CD, the recovered signal is required to be multiplied by $\frac{1}{H(\omega)}$, which can be written as

$$\frac{1}{H(\omega)} = \frac{\tau S_a(\omega\tau/2)}{s(\omega)} = \sum w_n e^{-jn\omega} \quad (13)$$

where w_n are tap coefficients which can be obtained using FFE based on LMS [24], [25] and RLS [26], [27] algorithms et al. For conventional FFE scheme based on LMS algorithm, the output of the equalized complex-valued symbols can be expressed as

$$\mathbf{y}(k) = \mathbf{w}(k)\mathbf{s}^T(k) \exp\left[-\mathrm{j}\hat{\theta}(k)\right] \quad (14)$$

where $\mathbf{s}(k)$ represents the k-th symbol of the received signal $\mathbf{s}$ and $\mathbf{w}(k)$ is the k-th symbol of the tap coefficient vector $\mathbf{w}$ and is updated as

$$\mathbf{w}(k+1) = \mathbf{w}(k) + \eta\mathbf{s}(k)[\mathbf{d}(k) - \mathbf{y}(k)] \exp\left[-\mathrm{j}\hat{\theta}(k)\right] \quad (15)$$

where η is the step size and $0<\eta<1$. $\mathbf{d}(k)$ is the k-th symbol of the desired output. $\hat{\theta}(k)$ represents the k-th symbol of the estimated phase information via CPE using the fourth power algorithm [28], which can be expressed as

$$\hat{\theta}(k) = \frac{1}{4}\arg\left(\frac{1}{M}\sum_M \mathbf{s}^4(k)\right) \quad (16)$$

where M is the length of the received signal $\mathbf{s}$ in frequency domain.

In this paper, to relax the dependence on carrier phase estimation within the equalization of the recovered complex-valued symbols and further reduce the computational complexity, we propose a novel FFE scheme based on LMS algorithm, where the output of the equalizer is written as

$$\mathbf{y}'(k) = \mathbf{w}^*(k)\mathbf{s}^T(k) \quad (17)$$

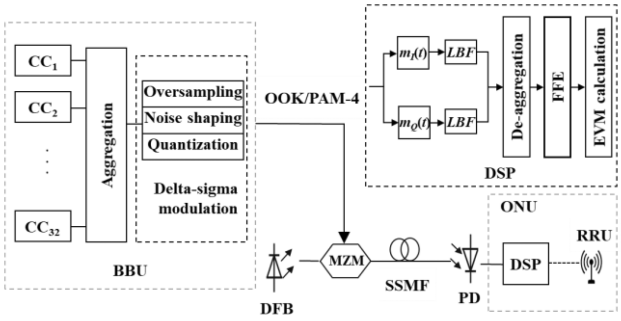

Fig. 3. Simulation setup of the MFH network using delta-sigma modulation.

Different from conventional FFE based on LMS algorithm, here $\mathbf{w}$ is initialized with complex values to enable the equalization for complex-valued signal directly. $\mathbf{w}*$ denotes the conjugation of $\mathbf{w}$, which is updated as

$$\mathbf{w}(k+1) = \mathbf{w}(k) + \eta\mathbf{s}(k)[\mathbf{d}(k) - \mathbf{y}'(k)]^* \quad (18)$$

Here to obtain quick and sufficient convergence, the tap coefficient vector is updated using the training sequence with length of 6000. After convergence, the update of the tap coefficient vector stops and the received signals are equalized by multiplying the latest tap coefficient vector directly.

III. Simulation and Results

A. Simulation Setup

Fig. 3 illustrates the simulation setup of the MFH network using delta-sigma modulation. At the baseband unit (BBU), 32 component carriers (CCs) of mobile signals with each bandwidth of 20 M are aggregated for DSP, in which respective 16 CCs1of 64QAM and 256QAM for 1-bit quantization and 10 CCs of 1024QAM and 22 CCs of 256QAM for 2-bit quantization are accommodated and all EVMs of them meet the specifications for 3GPP (1024QAM 1%, 256QAM 3.5% and 64QAM 8%) [33]. After that, the signals are fed into a delta-sigma modulator and up-sampled with sampling rate of 10.5 Gsa/s, in which the OSR of 8 is employed and digitalized into 10 Gbaud OOK signals by 1-bit quantization or PAM-4 signals by 2-bit quantization after noise shaping. Next, the generated PAM-4 signals are loaded onto a Mach-Zehnder Modulator (MZM) which is driven by a distributed feedback (DFB) laser with central wavelength of 1550 nm to generate optical signals for 30 km standard single-mode fiber (SSMF) transmission. The dispersion parameter of the SSMF is set as 17 ps/nm/km. At the optical network unit (ONU), the received signals are converted into photocurrent by a photodetector (PD). Prior to the RRH, the converted photocurrent is first split by a pair of matched filters $m_{\mathrm{I}}(\mathrm{t})$ and $m_{\mathrm{Q}}(\mathrm{t})$. After that low-pass filtering (LPF) is performed to filter out the quantization noise at the high-frequency domain. Next, the obtained data sequences are combined to format the original QAM symbols. The later DSP stage consists of a carrier de-aggregation process that de-aggrates the 32 CCs of digital signals for baseband processing followed by the FFE based on

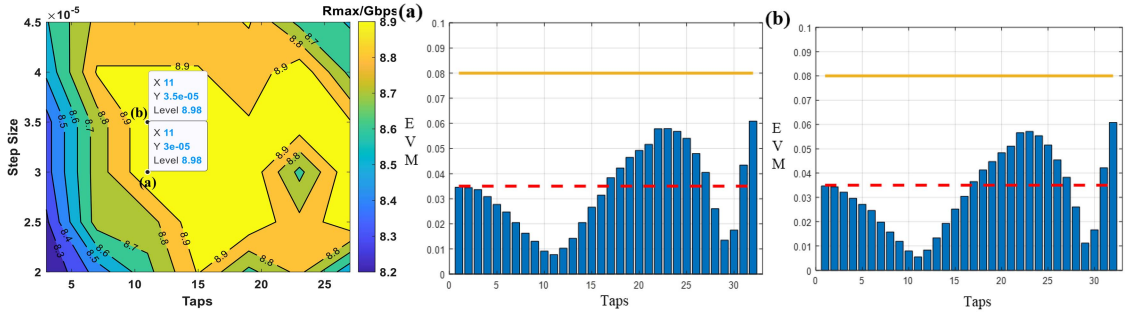

Fig. 4. Contour map for the maximum achievable capacity of different tap coefficients and iteration step sizes for the MFH network using delta-sigma modulator with 1-bit quantization and corresponding EVM distribution of the CCs.

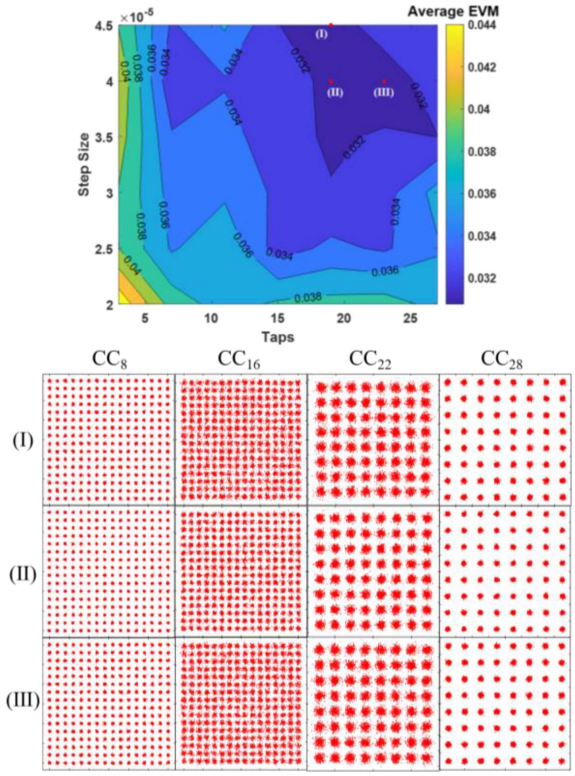

Fig. 5. Contour map for the EVM performance of different tap coefficients and iteration step sizes for the MFH network using delta-sigma modulator with 1-bit quantization and corresponding constellation diagrams of the recovered signals of the CCs.

LMS algorithm to mitigate the ISI. Finally, EVM calculation is operated to evaluate the whole system performance.

B. Results and Discussion

We first investigate the performance of the MFH network with delta-sigma modulator with 1-bit quantization. Fig. 4 shows the maximum achievable capacity of different tap coefficients and iteration step sizes for the MFH network with delta-sigma modulator. The maximum achievable capacity can be expressed

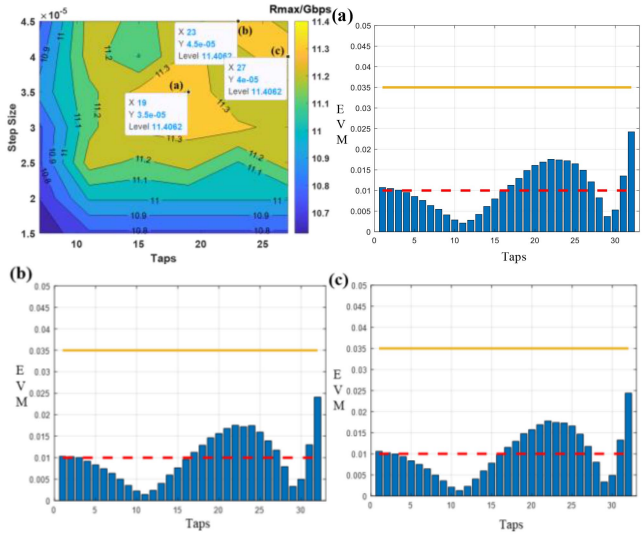

Fig. 6. Contour map for the maximum achievable capacity of different tap coefficients and iteration step sizes for the MFH network using delta-sigma modulator with 2-bit quantization and corresponding EVM distribution of the CCs.

as

$$R_{\max} = 2B_c \times (N_1 \log_2 M_1 + N_2 \log_2 M_2) \tag{19}$$

where B_c represents the bandwidth of each CC. $N_1$and N_2 is the number of the CCs of which the EVM meets the 3 GPP specification for 256QAM and 64QAM respectively. It can be found that the maximum transmission capacity of 8.98 Gbps (N_1 = 19 and N_2 = 13) can be achieved when the cases of (a) tap number: 11, step size: 3 × 10^{-5}; and (b) tap number: 11, step size: 3.5 × 10^{-5} are adopted. Also shown is the EVM distribution of the CCs of the aforementioned cases.

We also investigated the EVM performance of different tap coefficients and iteration step sizes for the MFH network with delta-sigma modulator with 1-bit quantization, which is shown in Fig. 5. It can be seen that the minimum average value of EVM less than 3.2% can be obtained when the cases of (I) tap number: 19, step size: 4.5 × 10^{-5}; (II) tap number: 19, step size: 4 × 10^{-5} and (III) tap number: 23, step size: 4 × 10^{-5} are adopted. Also shown is the constellation diagrams of the recovered signals of

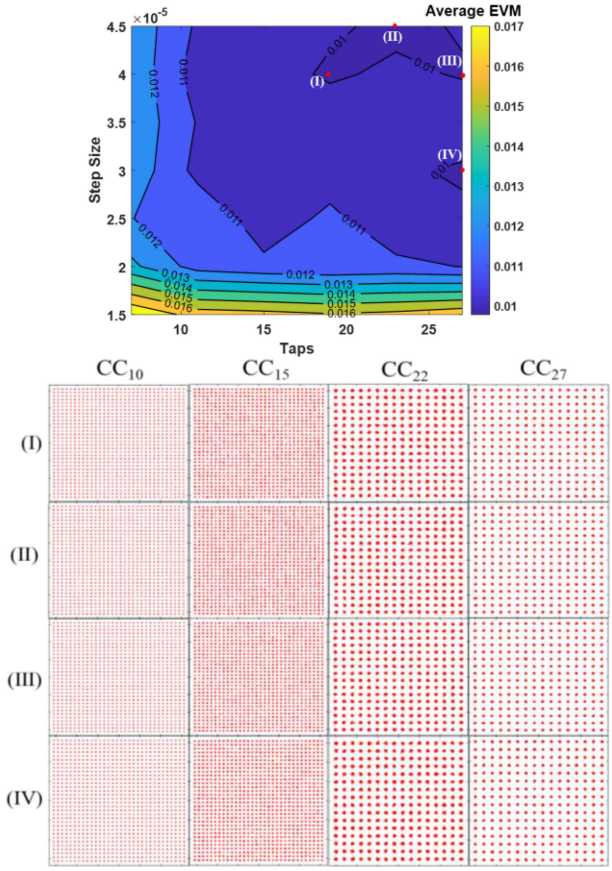

Fig. 7. Contour map for the EVM performance of different tap coefficients and iteration step sizes for the MFH network employing delta-sigma modulator with 2-bit quantization and corresponding constellation diagrams of the recovered signals of the CCs.

CC_8, CC_{16}, CC_{22} and CC28 with the cases (I)–(III) respectively. Since the required multiplications and additions/subtractions for LMS-based equalizer is $2N+1$ and $2N$ respectively within each iteration [34], where N is the tap length of the LMS-based equalizer, the computational complexity of the FFE scheme can be written as $O(N)$. The minimum average value of EVM with the minimum computational complexity can be achieved when employing the FFE scheme with 19 taps and step size of 4.5 × 10-5 or 4 × 10-5 as the computational complexity of FFE increases with the taps.

The performance of the MFH network employing delta-sigma modulator with 2-bit quantization is also investigated, where the maximum achievable capacity of different tap coefficients and iteration step sizes is presented in Fig. 6. Similarly to the case of 1-bit quantization, here the maximum achievable capacity can be written as

$$R'_{\max} = 2B_c \times (N_3 \log_2 M_3 + N_2 \log_2 M_2) \qquad (20)$$

where N_3 is the number of the CCs of which the EVM meets the 3GPP specification for 1024QAM. We can observe that the maximum transmission capacity of 11.4 Gbps corresponding to the case of $N_2 = 14$ and $N_3 = 18$ can be obtained when the cases of (a) tap number: 19, step size: 3.5 × 10^{-5}; (b) tap number: 23, step size: 4.5 × 10^{-5}; and (c) tap number: 27, step size: 4 × 10^{-5} are employed. We also illustrate EVM distribution of the CCs of the aforementioned cases in the respect inserts in Fig. 6. Since the computational complexity of FFE increases with the taps, the maximum transmission capacity with the minimum computational complexity can be obtained when the tap length of the FFE scheme is 19 and the step size is 3.5 × 10^{-5}.

The EVM performance of different tap coefficients and iteration step sizes for the MFH network employing delta-sigma modulator with 2-bit quantization is depicted in Fig. 7, where the minimum average value of EVM less than 1% can be obtained when the cases of (I) tap number: 19, step size: 4 × 10^{-5}; (II) tap number: 23, step size: 4.5 × 10^{-5}; (III) tap number: 27, step size: 4 × 10^{-5} and (IV) tap number: 27, step size: 3 × 10^{-5} are adopted. Also shown is the constellation diagrams of the recovered signals of CC_{10}, CC_{15}, CC_{22} and CC_{27} with the cases (I)–(IV) respectively. The minimum average value of EVM with the minimum computational complexity can be obtained when case (I) is adopted, since the computational complexity of FFE increases with the tap length as described previously.

IV. Conclusion

In conclusion, to mitigate ISI issue in MFH networks based on delta-sigma modulation technology, we have proposed a novel LMS based FFE scheme for MFH networks employing 4th-order delta-sigma modulator with both 1-bit and 2-bit quantization. The number of taps and step size of the FFE has been systematically studied to achieve the optimal performance. Results show that, for the lowest computational complexity, the maximum transmission capacity of 8.98 Gbps can be obtained when employing the FFE scheme with 11 taps and step size of 3 × 10^{-5} or 3.5 × 10^{-5} and the minimum average EVM less than 0.032 can be achieved with 19 taps and step size of 4 × 10^{-5} or 4.5 × 10^{-5} for 1-bit quantization system. For 2-bit quantization system, the maximum transmission capacity reaches 11.4 Gbps when the tap length of the FFE is 19 and step size is 3.5 × 10^{-5} while the minimum average EVM less than 0.01 can be obtained with 19 taps and step size of 4 × 10^{-5}. Based on the results, we believe our study can provide guidelines for selecting an optimal equalization scheme based on the integrated requirements of EVMs, capacity and computational complexity.

References

[1] A. Pizzinat, P. Chanclou, F. Saliou, and T. Diallo, "Things you should know about fronthaul," *J. Lightw. Technol.*, vol. 33, no. 5, pp. 1077–1083, Mar. 2015.
[2] J. I. Kani, S. Kaneko, K. Hara, and T. Yoshida, "Optical access network evolution for future super-broadband services and 6G mobile networks," in *Proc. Eur. Conf. Opt. Commun.*, 2021, pp. 1–4.
[3] T. Pfeiffer, "Next generation mobile fronthaul and midhaul architectures," *J. Opt. Commun. Netw.*, vol. 7, pp. B38–B45, 2015.
[4] D. Wake, A. Nkansah, and N. J. Gomez, "Radio over fiber link design for next generation wireless systems," *J. Lightw. Technol.*, vol. 28, no. 16, pp. 2456–2464, Aug. 2010.
[5] X. Liu, H. Zeng, N. Chand, and F. Effenberger, "Efficient mobile fronthaul via DSP-based channel aggregation," *J. Lightw. Technol.*, vol. 34, no. 6, pp. 1556–1564, Mar. 2016.
[6] P. Banelli and S. Cacopardi, "Theoretical analysis and performance of OFDM signals in nonlinear AWGN channels," *IEEE Trans. Commun.*, vol. 48, no. 3, pp. 430–441, Mar. 2000.

[7] "Common public radio interface (CPRI): Interface specification," CPRI Specification V 7.0, Oct. 2015. [Online]. Available: http://www.cpri.info/downloads/CPRI_v_7_0_2015-10-09.pdf

[8] A. d. l. Oliva, J. A. Hernandez, D. Larrabeiti, and A. Azcorra, "An overview of the CPRI specification and its application to C-RAN-based LTE scenarios," *IEEE Commun. Mag.*, vol. 54, no. 2, pp. 152–159, Feb. 2016.

[9] K. Bai et al., "Digital mobile fronthaul based on performance enhanced multi-stage noise-shaping delta-sigma modulator," *J. Lightw. Technol.*, vol. 39, no. 2, pp. 439–447, Jan. 2021.

[10] J. Wang, Z. Jia, L. A. Campos, and C. Knittle, "Delta-sigma modulation for next generation fronthaul interface," *J. Lightw. Technol.*, vol. 37, no. 12, pp. 2838–2850, Jun. 2019.

[11] J. Wang et al., "Delta-sigma modulation for digital mobile fronthaul enabling carrier aggregation of 32 4G-LTE /30 5G-FBMC signals in a single-λ 10-Gb/s IM-DD channel," in *Proc. Opt. Fiber Commun. Conf.*, 2016, pp. 1–3.

[12] J. Wang et al., "Digital mobile fronthaul based on delta–sigma modulation for 32 LTE carrier aggregation and FBMC signals," *J. Opt. Commun. Netw.*, vol. 9, 2017, Art. no. A233.

[13] J. Wang, Z. Jia, L. A. Campos, L. Cheng, C. Knittle, and G.-K. Chang, "Delta-sigma digitization and optical coherent transmission of DOCSIS 3.1 signals in hybrid fiber coax networks," *J. Lightw. Technol.*, vol. 36, no. 2, pp. 568–579, Jan. 2018.

[14] Z. Chen et al., "4 × 32-Gbps block-wise QPSK 1200-km SSMF direct detection transmission based on delta-sigma virtual carrier generation," *IEEE Photon. J.*, vol. 11, no. 6, Dec. 2019, Art. no. 7907407.

[15] Y. Wei et al., "PDM-OFDM 1-bit DSM 1024QAM/4096QAM signals at W-band transmission over 4.6-km wireless distance," *Opt. Lett.*, vol. 48, no. 17, pp. 4448–4451, 2023.

[16] Y. Zou et al., "A hierarchical modulation enabled SNR allocable delta-sigma digital mobile fronthaul system," *IEEE Photon. J.*, vol. 14, no. 1, Feb. 2022, Art. no. 7905406.

[17] H. Li et al., "Improving performance of mobile fronthaul architecture employing high order delta-sigma modulator with PAM-4 format," *Opt. Exp.*, vol. 25, no. 1, pp. 1–9, 2017.

[18] L. Zhong et al., "An SNR-improved transmitter of delta-sigma modulation supported ultra-high-order QAM signal for fronthaul/WiFi applications," *J. Lightw. Technol.*, vol. 40, no. 9, pp. 2780–2790, May 2022.

[19] K. Bai et al., "Digital mobile fronthaul based on performance enhanced multi-stage noise-shaping delta-sigma modulator," *J. Lightw. Technol.*, vol. 39, no. 2, pp. 439–447, Jan. 2021.

[20] Y. Zhu, L. Yin, Q. Wu, L. Man, Y. Tao, and W. Hu, "Up to 16384-QAM IFoF transmission with DML based on 2-bit high-pass delta-sigma modulation," in *Proc. Asia Commun. Photon. Conf.*, 2021, Paper T3B.6.

[21] A. Lowery and J. Armstrong, "Orthogonal-frequency-division multiplexing for dispersion compensation of longhaul optical systems," *Opt. Exp.*, vol. 14, pp. 2079–2084, 2006.

[22] A. Leven, N. Kaneda, and Y. K. Chen, "A real-time CMA-based 10 Gb/s polarization demultiplexing coherent receiver implemented in an FPGA," in *Proc. Conf. Opt. Fiber Commun./Nature. Fiber Opt. Engineers Conf.*, 2008, Paper OTuO2.

[23] Y. Wang, L. Tao, Y. Wang, and N. Chi, "High speed WDM VLC system based on multi-band CAP64 with weighted pre-equalization and modified CMMA based post-equalization," *IEEE Commun. Lett.*, vol. 18, no. 10, pp. 1719–1722, Oct. 2014.

[24] S. Randel et al., "6 × 56-Gb/s mode-divisionmultiplexed transmission over 33-km few-mode fiber enabled by 6 × 6 MIMO equalization," *Opt. Exp.*, vol. 19, no. 17, pp. 16697–16707, 2011.

[25] R. Ryf et al., "Mode-division multiplexing over 96 km of few-mode fiber using coherent 6 × 6 MIMO processing," *J. Lightw. Technol.*, vol. 30, no. 4, pp. 521–531, Feb. 2012.

[26] Y. Wang, X. Huang, L. Tao, J. Shi, and N. Chi, "4.5-Gb/s RGB-LED based WDM visible light communication system employing CAP modulation and RLS based adaptive equalization," *Opt. Exp.*, vol. 23, no. 10, pp. 13626–13633, 2015.

[27] K. Bandara and Y. H. Chung, "Reduced training sequence using RLS adaptive algorithm with decision feedback equalizer in indoor visible light wireless communication channel," in *Proc. IEEE Int. Conf. ICT Convergence*, 2012, pp. 149–154.

[28] A. J. Viterbi and A. M. Viterbi, "Nonlinear estimation of PSK-modulated carrier phase with application to burst digital transmission," *IEEE Trans. Inf. Theory*, vol. 29, no. 4, pp. 543–551, Jul. 1983.

[29] R. Schreier and G. C. Temes, *Understanding Delta-Sigma Data Converters*. Hoboken, NJ, USA: Wiley, 2004.

[30] D. Tan et al., "A novel structure optimizer based on heuristic search for delta-sigma modulator in mobile fronthaul," *IEEE Photon. Technol. Lett.*, vol. 34, no. 21, pp. 1131–1134, Nov. 2022.

[31] D. Tan et al., "A novel structure design method of delta-sigma modulator based on genetic algorithm for mobile fronthaul," in *Proc. Opt. Fiber Commun. Conf.*, 2022, pp. 1–3.

[32] H. Yao et al., "Experimental demonstration of 4-PAM for high-speed indoor free-space OW communication based on cascade FIR-LMS adaptive equalizer," *Opt. Commun.*, vol. 23, no. 10, pp. 13626–13633, 2018.

[33] 3rd Generation Partnership Project, "Base station (BS) radio transmission and reception," 3GPP, Sophia Antipolis, France, Tech. Specification 36.104, Feb. 2015.

[34] J. Li, C. Lim, and A. Nirmalathas, "Comparison of adaptive equalization methods for improving indoor optical wireless communications employing few-mode based uniform beam shaping," *J. Lightw. Technol.*, vol. 40, no. 12, pp. 3768–3776, Jun. 2022.